DOI: 10.13009/EUCASS2017-601

7TH EUROPEAN CONFERENCE FOR AERONAUTICS AND AEROSPACE SCIENCES (EUCASS)

DOI: ADD DOINUMBER HERE

Modeling, numerical method and validation for the simulation of hypersonic rarefied gas flows

C Baranger[⋆†], *L. Desvillettes*[◇], *N. Hérouard*[⋆], *J. Mathé*[⋆], *J. Mathiaud*[⋆], *J.F. Poustis*[⋆], *L. Mieussens*[*], *M. Varenne-Pellegrini*[⋆]

[⋆] *CEA-CESTA 15 avenue des Sablières CS 60001 33116 Le Barp Cedex France*
[*] *Institut de Mathématiques de Bordeaux (UMR 5251), Univ. Bordeaux, 351, cours de la libération, 33405 Talence France*
[◇] *Université Pierre et Marie Curie-Université Paris Diderot (UMR 7586) 75013 Paris France*

celine.baranger@cea.fr · laurent.desvillettes@imj-prg.fr · nicolas.herouard@gmail.com · jordane.mathe@cea.fr
julien.mathiaud@cea.fr · jean-francois.poustis@orange.fr · Luc.Mieussens@math.u-bordeaux.fr · marielle.varenne@cea.fr
[†]Corresponding author

Abstract

To compute parietal flux and aerodynamic coefficients of space shuttles, one has to simulate precisely hypersonics flows around them. In the upper layers of the atmosphere, the air is in a rarefied state and described by Boltzmann-like equation. We develop a BGK model for real gas (polyatomic, with small Prandtl number, with chemical reactions) to simulate such flows. The deterministic numerical method (second order) used to achieve simulation in 2D and 3D is compatible with diffuse boundary conditions. The simulations are compared with experiments made at the MARHy facility (ex. SR3) of the ICARE CNRS Laboratory at Orleans.

1. Introduction

During re-entry of space shuttle, various kind of atmospheric layers are encountered at high speed. To develop such shuttles, one has to compute parietal flux and aerodynamic coefficients on these objects, which implies to simulate precisely air flows around them. In the upper layers of the atmosphere, the air is in a rarefied state, the mean free path of the particles of air is not so small as compared to the size of the shuttle. In such a rarefied regime, the Knudsen number which is the ratio between the mean free path λ and a characteristic length L ($Kn = \frac{\lambda}{L}$) is larger than 0.01, and is used to discriminate rarefied regime from continuous regime (at low altitude) and also from the molecular regime (very high altitude). In the continuous regime, the flow is described by the compressible Navier-Stokes equations of Gas Dynamics. In the molecular regime, the Newton law is used to describe quantities at the boundary of the shuttle. In the rarefied regime, the Navier-Stokes equations are no longer valid and the use of the kinetic theory of gas *via* the Boltzmann equation is needed. The evolution of the molecules of the gas is then described by a mass density distribution in phase space, which is a solution of the Boltzmann equation. In the transitional regime (from rarefied to the beginning of continuous regime), this equation can be replaced by the simpler Bhatnagar-Gross-Krook (BGK) model: the complex collision term of the Boltzmann equation is replaced by a relaxation toward the equilibrium. This model is simpler than the Boltzmann equation but keeps the same conservation properties. However, it relies on a simple gas model (monoatomic for example).
The most popular numerical method to simulate rarefied flows is the Direct Simulation Monte Carlo method (DSMC).[6] However, it is well known that this method is very expensive in transitional regimes, in particular for flows in the range of altitude we are interested in here. In contrast, deterministic methods (based on a numerical discretization of the stationary kinetic model) can be more efficient in transitional regimes. In our team at the CEA (French Atomic Energy Agency), we developed several years ago a deterministic code to make 2D plane and axisymmetric simulations of rarefied flows based on the BGK model. This code has been extended to 3D computations, for polyatomic gases. The BGK model is approximate with a discrete velocity method and a deterministic solver. A finite volume scheme is used to achieve stationary computations (see[3,12,13]).
Due to the physical model (polyatomic gases), the space discretization (block structured mesh), and the parallelisation (space domain decomposition with MPI and inner parallelisation with openMP), this code is rather different from the other existing 3D codes recently presented in the literature for the same kind of problems (the 3D code of Titarev[15]

DOI: 10.13009/EUCASS2017-601

for example). In order to be able to achieve realistic simulations (3D configurations with Mach number larger than 20), the method to discretize the velocity space has to be modified in order to decrease CPU time and memory storage requirements. We presented recently[4,5] our new strategy to reduce the cost of computation: the locally refined discrete velocity grids. The use of this AMR (Adaptative Mesh Refinement) velocity grid was a significative improvement in term of computational cost. With such strategy, realistic computations (3D and high Mach number) are now available. In order to be able to treat realistic configurations, the BGK-model was updated. It is well known that the BGK equation leads to a Prandtl number (ratio between viscous effect to thermal effect) equal to 1. We present here the ES-BGK model (described in[2]) which enables realistic Prandtl number and the extension of this model to polyatomic gases.
We also deal with some evolutions of the BGK model for more complex gas (with small Prandtl number, with chemical reactions) and the numerical method of second order used to achieve simulation in 2D and 3D. We will pay attention to the order of accuracy of the method, by computing the correct boundary conditions with respect to the scheme and detail the validation of the code by comparison with test cases from literature. Finally, we will present the comparison of simulation of rarefied flows with experiments made at the MARHy facility (ex. SR3) of the ICARE CNRS Laboratory at Orleans.

2. Kinetic Model for hypersonic rarefied flows

In the rarefied regime, the molecules of the gas in the flow are described by the distribution function $f \equiv f(t, \mathbf{x}, \mathbf{v})$ depending on time t, position $\mathbf{x} \in \mathbb{R}^3$ and speed $\mathbf{v} \in \mathbb{R}^3$. This function is the solution of the Boltzmann equation.

2.1 BGK model

As we are interested in the transitional regime, where the Knudsen number is between 0.01 to 1, we use here the Bathnagar, Gross, et Krook model (BGK). The collision term of the Boltzmann equation is replaced by a relaxation toward equilibrium:

$$\frac{\partial f}{\partial t} + \mathbf{v} \cdot \nabla_{\mathbf{x}} f = \frac{1}{\tau}(\mathcal{M}(f) - f) \tag{1}$$

The first part of the equation solves the moving state of the particles, and the right hand side of the equation is the relaxation toward the equilibrium $\mathcal{M}(f) = \frac{\rho}{(2\pi RT)^{3/2}} e^{\frac{-|\mathbf{v}-\mathbf{u}|^2}{2RT}} = \mathcal{M}(\rho, \mathbf{u}, T)$, called a Maxwellian. Here, the macroscopic quantities ρ, $\mathbf{u}$ and T, depending on time and space, are related to the first three moments of the distribution function f. The relaxation rate $\tau = \tau(t, \mathbf{x})$ depends on macroscopic quantities of the flow like pressure and viscosity.
This equation is supplemented by boundary conditions. Far from the boundary of the flying object, the distribution function is determined with the characteristic of the atmosphere (pressure and density), and with the velocity of the object (we compute in the relative referential). At the boundary of the object, several conditions can be applied: diffusive reflexion of the particules on the wall, specular reflection or mixed condition with an accommodation coefficient. This coefficient is supposed to be related to the state of the surface of the body. It is still a chalenge to determine precisely the value of this coefficient.
The BGK model preserves the mass, momentum and kinetic energy of the particles and the entropy dissipation (H-theorem). By integrating the distribution function with respect to the velocity $\mathbf{v}$, we define the macroscopic quantities $\rho, \mathbf{u}, \mathbf{T}$:

$$\begin{pmatrix} \rho \\ \rho\mathbf{u} \\ \frac{3}{2}\rho RT \end{pmatrix} = \int_{\mathbf{v}} \begin{pmatrix} f(t, \mathbf{x}, \mathbf{v}) \\ \mathbf{v}\, f(t, \mathbf{x}, \mathbf{v}) \\ \frac{1}{2}|\mathbf{v} - \mathbf{u}|^2 f(t, \mathbf{x}, \mathbf{v}) \end{pmatrix} d\mathbf{v} \tag{2}$$

When the Knudsen number tends to 0 (i.e. the continuous regime), the macroscopic quantites (ρ, $\rho\mathbf{u}$, ρT) are solution of the asymptotic limit of the BGK model: the Navier-Stokes equations. We are then able to compare the solutions of the two systems, the macroscopic quantities issued fom the rarefied solution of the BGK model and the solution of the Navier-Stokes equations.
We plot on the figure 1 the pressure, temperature and Mach number for a flow around a sphere of 0.1 m diameter. The flow is at Mach 5, pressure $22.14 Pa$ and density $3.14\, 10^{-4} kg.m^{-3}$ (approximatively 60 km altitude). The Knudsen number is then of order 2.10^{-3}, and is small enough so that the continuous and rarefied solutions are close. On the figure 1, we plot the pressure, temperature and Mach number for the Navier-Stokes (bottom) and BGK solution (top). The macroscopic quantities are then very close. We have to mention here that the Navier-Stokes solution was obtained with the fixed Pr parameter equal to 1 and that the flow is consider to be a perfect gas, with classical viscosity for air (see subsection 2.2).

DOI: 10.13009/EUCASS2017-601

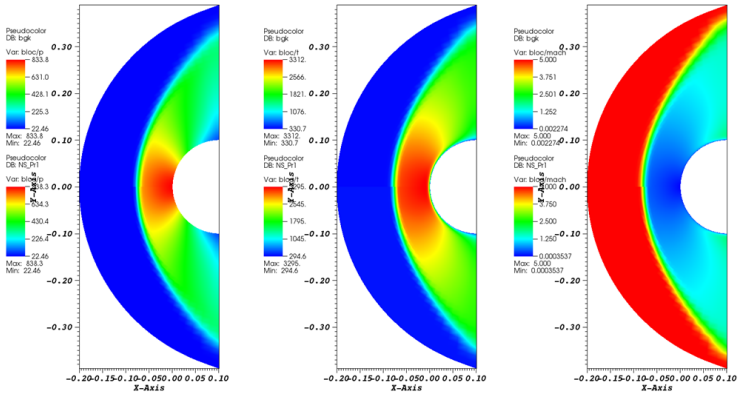

Figure 1: The pressure, temperature and Mach number between BGK solution (top) and Navier-Stokes solution (bottom) for a flow at Mach 5 and Knusden 2.10^{-3}

2.2 BGK-like models to describe atmospheric flow

To describe the air surrounding space shuttle during reentry, the BGK model has to be adapted to deal with real flow. The relaxation rate obtained by a Chapmann-Enskog expansion from the Boltzmann model, is equal to:[6]

$$\tau = \frac{\mu}{P} = \frac{1}{P}\mu_{ref}\left(\frac{T}{T_{ref}}\right)^{\omega}, \tag{3}$$

where $\omega = 0.77$, $T_{ref} = 273K$, $\mu_{ref} = 1.719\,10^{-5}\,N.s.m^{-2}$.
The gas in earth atmosphere is air which is composed by diatomic molecules (N_2 and O_2). The BGK model described above is dedicated to the description of monoatomic molecules (no additional parameters to deal with internal energy of the molecules). The extension[9]of this model for polyatomic molecules has been made. The internal energy is an additional variable of the distribution function, and by the use of the reduced distribution technique, a system of two BGK equations is obtained.
The main drawback of the BGK model is that the viscous and thermic effects are not independent, so that realistic values of the transport coefficients (Prandtl number, second viscosity) are not achievable. The BGK model describe for example flow with Prandtl number equal to 1. But, air flows have Prantdl number arround 0.72. The heat flux at the boundary is then underestimated with the classical BGK model. The ES-BGK model presented in ([2,10]) gives the correct transport coefficients and Prandtl number.
Finally, as the temperature that occur in front of the wall can be very high (between 1000K to 6000K), the N_2 and O_2 molecules of the air will undergo chemical reactions, and the N, O and NO species will appear, and it will decrease the macroscopic temperature of the flow and the heat flux at the boundary. We will present in subsection 2.5 a model that take into account the effect of chemical reactions on a ES-BGK model.

2.3 ES-BGK model for real Prandtl number and monoatomic gas

The idea of the Ellipsoïdal Statistical model is to replace the Maxwellian function $\mathcal{M}$ by a Gaussian function $\mathcal{G}$, and the temperature, by a tensor of temperature $\mathcal{T}$.

$$\frac{\partial f}{\partial t} + \mathbf{v}\cdot\nabla_{\mathbf{x}} f = \frac{1}{\tau}(\mathcal{G}(\rho,\mathbf{u},\mathcal{T}) - f) \tag{4}$$

with $\mathcal{G}(\rho,\mathbf{u},\mathcal{T}) = \frac{\rho}{\sqrt{\det(2\pi\mathcal{T})}} e^{\frac{-(\mathbf{v}-\mathbf{u})\mathcal{T}^{-1}(\mathbf{v}-\mathbf{u})}{2}}$ and

$$\tau = \frac{\mu}{Pr\,\rho\,R\,T}.$$

The tensor of temperature is defined by $\mathcal{T} = (1-\nu)RT\mathbf{I}d + \nu\Theta$, where $\Theta = \frac{1}{\rho}\int(\mathbf{v}-\mathbf{u})\otimes(\mathbf{v}-\mathbf{u})f$ and the macroscopic temperature still determined by $T = \frac{1}{3\rho R}\int_{\mathbf{v}}|\mathbf{v}-\mathbf{u}|^2 f d\mathbf{v}$.

DOI: 10.13009/EUCASS2017-601

The Prandtl number is obtain by a Chapmann-Enskog expansion

$$Pr = \frac{1}{1-\nu} \tag{5}$$

Then, for a monoatomic gas with $\nu = -0.5$, we recover the classical value $Pr = \frac{2}{3}$. The classical BGK model is included in the ES-BGK model as it corresponds to the value $\nu = 0$.
On figure 2.3, we present the result of the ES-BGK model with $Pr = 2/3$ and compare it to the previous solution of BGK ($Pr = 1$) and with Navier-Stokes ($Pr = 1$ and $2/3$). We have good agreement between the solutions with same Prandtl number. This ensures the validity of the ES-BGK model for monoatomic gases.

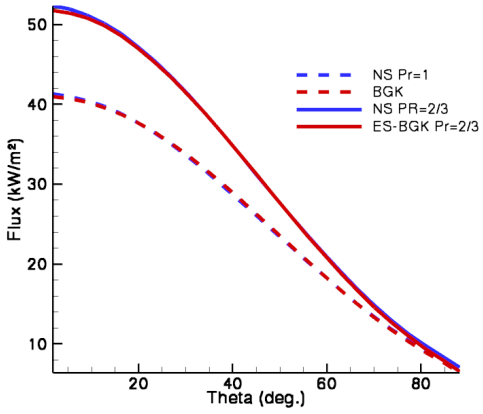

Figure 2: Comparison between Navier-Stokes ($Pr = 1$ and $2/3$), BGK and ES-BGK

2.4 ES-BGK model for polyatomic gases (Air, Nitrogen, etc...)

When we are interested in simulate reentry in atmosphere composed by air, the model of ES-BGK presented previously is not suitable to describe polyatomic gas. An extension of the BGK model was proposed[9] by the use of the reduction technic and we extend this model in order to take into account a non equal to 1 Prandtl number. The idea of the model for polyatomic gas is the following : a new variable has te be added in the definition of the density function $f \equiv f(t, \mathbf{x}, \mathbf{v}, I)$ where I is the internal energy. When collisions occur between polyatomic molecules, the total energy (kinetic and internal energies) is conserved and not only the kinetic energy : a part of the kinetic energy will be transformed into internal energy (rotational or vibrational energy). The problem of this method is that it adds a new variable in the phase space and that its numerical solving is much more expensive. The reduced distribution technique consists in solving only the first two moments of f in the I variable: $\tilde{f} = \int_0^{+\infty} f(t, \mathbf{x}, \mathbf{v}, I)\, dI$ and $\tilde{g} = \int_0^{+\infty} I^{2/\delta} f(t, \mathbf{x}, \mathbf{v}, I)\, dI$. δ is the degree of freedom of the gas ($\delta = 2$ for diatomic gases). These two functions are solutions of the closed system of BGK equations:

$$\begin{aligned} \frac{\partial \tilde{f}}{\partial t} + \mathbf{v} \cdot \nabla_{\mathbf{x}} \tilde{f} &= \frac{1}{\tau}(\mathcal{M}(\rho, \mathbf{u}, T) - \tilde{f}) \\ \frac{\partial \tilde{g}}{\partial t} + \mathbf{v} \cdot \nabla_{\mathbf{x}} \tilde{g} &= \frac{1}{\tau}(\frac{\delta RT}{2}\mathcal{M}(\rho, \mathbf{u}, T) - \tilde{g}) \end{aligned}$$

By now, we will denote $\tilde{f}$ by f and $\tilde{g}$ by g.
Like in the ES-BGK model for monoatomic gas, a correct Prandtl number can be obtained by replacing the Maxwellian function $\mathcal{M}(\rho, \mathbf{u}, T)$ by a anisotropic Gaussian function $\mathcal{G}(\rho, \mathbf{u}, \mathcal{T})$:

$$\begin{aligned} \frac{\partial f}{\partial t} + \mathbf{v} \cdot \nabla_{\mathbf{x}} f &= \frac{1}{\tau}(\mathcal{G}(\rho, \mathbf{u}, \mathcal{T}) - f) \\ \frac{\partial g}{\partial t} + \mathbf{v} \cdot \nabla_{\mathbf{x}} g &= \frac{1}{\tau}(\frac{\delta RT_{rel}}{2}\mathcal{G}(\rho, \mathbf{u}, \mathcal{T}) - g) \end{aligned}$$

DOI: 10.13009/EUCASS2017-601

with $T_{rel} = \theta T + (1-\theta)T_{int}$ and $T_{tr} = \frac{1}{3\rho R}\int_{\mathbf{v}} |\mathbf{v}-\mathbf{u}|^2 f d\mathbf{v}$ $T_{int} = \frac{1}{\delta\rho R}\int_{\mathbf{v}} g d\mathbf{v}$, $T = \frac{3}{3+\delta}T_{tr} + \frac{\delta}{3+\delta}T_{int}$, and the tensor of temperature $\mathcal{T}$ depends on two parameters (θ, ν).

$$\mathcal{T} = (1-\theta)\left((1-\nu)RT_{tr}\mathbf{I}d + \nu\Theta\right) + \theta RT\mathbf{I}d$$

Then, the Prandtl number is

$$Pr = \frac{1}{1-(1-\theta)\nu}$$

With $\nu = -0.5, \theta = \frac{1}{5}$, we recover the Prandtl number for perfect polyatomic gas : $Pr = \frac{5}{7}$. For air, the Prandtl number is estimated at $Pr = 0.72$. The exchange of energy between translational and internal modes is driven by the parameter θ, which is adjusted by the formula of Lordi and Park[6] : $\theta = \frac{1}{Z_{rot}(T)}$.

2.5 Modeling of the chemical reaction for ES-BGK model

We will present here the modeling of the chemical reaction in the ES-BGK model for polyatomic molecules. During atmospheric reentry, temperatures in front of the object can be very high and polyatomic molecules of the air (N_2 and O_2) can be dissociated into N and O species. Recombinaison of these species can give NO specie. These reactions are endothermic and the global temperature will decrease. The heat flux flux at the wall will also decrease. In order to take into account such phenomena into our ES-BGK model for polyatomic gas, we construct a simple model that can be added easily in our numerical code : we choose not to solve the kinetic evolution of all the species, but only the kinetic evolution of N_2 and O_2 (majority species), and we describe the 3 other species N, O and NO with macroscopic quantities and equations (minority species). This model was made[8] to recover the same transport coefficients (viscosity, conductivity) as in the Navier-Stokes model with chemical reactions. The evolution of the minority species (O, N, NO) is described by the macroscopic equations:

$$\begin{aligned}
\frac{\partial \rho_O}{\partial t} + \nabla_{\mathbf{x}}\cdot\left(\rho_O\,\mathbf{u} + \rho D(T)\nabla_{\mathbf{x}}(\frac{\rho_O}{\rho})\right) &= \dot{\omega}_O(T)\\
\frac{\partial \rho_N}{\partial t} + \nabla_{\mathbf{x}}\cdot\left(\rho_N\,\mathbf{u} + \rho D(T)\nabla_{\mathbf{x}}(\frac{\rho_N}{\rho})\right) &= \dot{\omega}_N(T)\\
\frac{\partial \rho_{NO}}{\partial t} + \nabla_{\mathbf{x}}\cdot\left(\rho_{NO}\,\mathbf{u} + \rho D(T)\nabla_{\mathbf{x}}(\frac{\rho_{NO}}{\rho})\right) &= \dot{\omega}_{NO}(T)
\end{aligned}$$

where $\dot{\omega}_{O,N,NO}(T)$ are the source terms of the chemical reactions, which are the same as in a Navier-Stokes model with chemical reactions.
We present here two models of ES-BGK type with chemical reaction. The first take into account a new temperature, but its main drawback is that there is a free parameter that we cannot estimate. We propose then a second model, in which there is not free parameter.
First model:

$$\begin{aligned}
\frac{\partial f}{\partial t} + \mathbf{v}\cdot\nabla_{\mathbf{x}} f &= \frac{1}{\tau}(\mathcal{G}(\rho,\mathbf{u},\mathcal{T}) - f) + \frac{1}{\hat{\tau}}(\mathcal{M}(\rho,\mathbf{u},\hat{\mathcal{T}}) - f)\\
\frac{\partial g}{\partial t} + \mathbf{v}\cdot\nabla_{\mathbf{x}} g + \beta g &= \frac{1}{\tau}(\frac{\delta RT_{rel}}{2}\mathcal{G}(\rho,\mathbf{u},\mathcal{T}) - g)
\end{aligned}$$

where $\hat{\tau}$ is a relaxation time, $\hat{T} = (1-\beta\hat{\tau})T_{int}$ is the modified temperature and $\beta(T,\rho,\rho_O,\rho_N,\rho_{NO})$ is the transfer coefficient between internal and chemical energies.
Second model:

$$\begin{aligned}
\frac{\partial f}{\partial t} + \mathbf{v}\cdot\nabla_{\mathbf{x}} f + \frac{\beta}{2}\nabla_{\mathbf{v}}\cdot\left((\mathbf{u}-\mathbf{v})\mathcal{M}(\rho,\mathbf{u},T)\right) &= \frac{1}{\tau}(\mathcal{G}(\rho,\mathbf{u},\mathcal{T}) - f)\\
\frac{\partial g}{\partial t} + \mathbf{v}\cdot\nabla_{\mathbf{x}} g + \beta\frac{\delta RT_{rel}}{2}\mathcal{M}(\rho,\mathbf{u},T) &= \frac{1}{\tau}(\frac{\delta RT_{rel}}{2}\mathcal{G}(\rho,\mathbf{u},\mathcal{T}) - g)
\end{aligned}$$

where $\beta(T,\rho,\rho_O,\rho_N,\rho_{NO})$ is the transfer coefficient between internal and chemical energies.
These two models were implemented in the kinetic code at CEA and compared with a Navier-Stokes simulation with chemical reactions. We are able to compare the evolution of the minority species, the macroscopic temperature of the flow and the heat flux (figure 3) at the boundary in a simulation with or without chemical reactions. The second model seems to be closer to the Navier-Stokes solution and more investigations on this model will be needed.

DOI: 10.13009/EUCASS2017-601

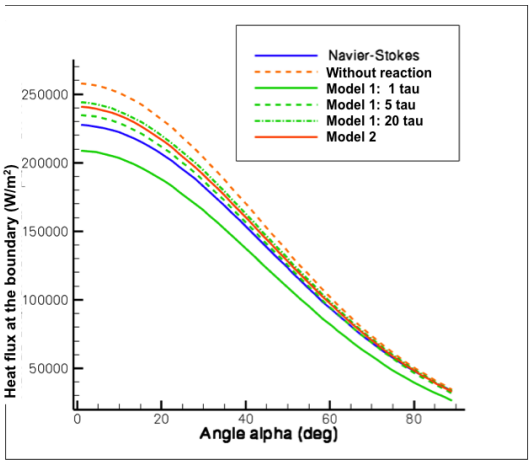

Figure 3: Heat flux for Navier-Stokes simulation with chemical reactions, BGK model without chemical reaction, and model 1 ($\hat{\tau} = \tau, 5\,\tau$ or $20\,\tau$) and model 2

3. Numerical method of second order

The models presented previously are solved numerically with a deterministic method: a finite volume method for the discretization in space variable and a discrete velocity model[13] for the velocity variable. In order to decrease the cost of simulations, and particularly to be able to make 3D simulations in hypersonic reentry, some innovative methods were developed. The discretization of the velocity space was adapted and an adaptative mesh refinement[5] was implemented. The gain is between 7 to 25 in 2D, 25 to 150 in 3D.
The discretization in space was also improved: in our first version, we used a standard second order finite volume scheme (based on the Yee flux limiter[16]), see.[5] We observed that the second order of the scheme was not preserved up to the solid wall. We replaced the flux limiter by a slope limiter with a linear reconstruction to compute it. The boundary condition was adapted to this slope limiter scheme, and the order of the scheme was found to be higher with this method than with the flux limiter method (figure 4)

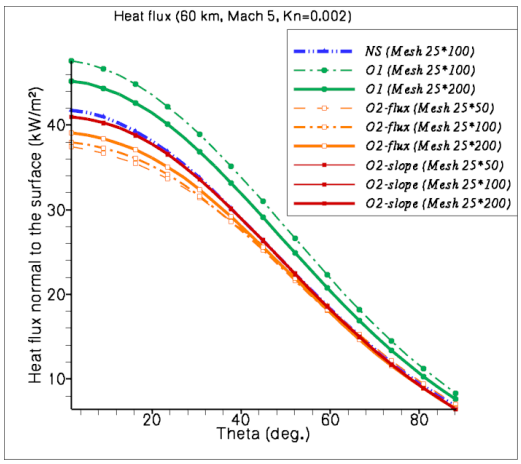

Figure 4: 2D supersonic flow: comparison of the heat flux between BGK solved with finite volume schemes (O1, O2-flux, O2-slope) for different meshes, and Navier-Stokes (NS)

4. Comparison with a DSMC code

We validated our model and numerical method by comparison with experimental data and also with a code based on the DSMC (Direct Simulation Monte Carlo) method. In[11] the DSMC code MONACO (Univ. Michigan) was used. The

DOI: 10.13009/EUCASS2017-601

characteristics of the test case are detailed in the table 1 and geometry in figure 5.

For this test case, the DSMC code MONACO is used with 20000 cells in space, 7.10^6 particles, 430000 iterations on 32 processors. For the BGK code, 200000 mesh in space, 20000 points in the velocity grid, 500 iterations on 1000 processors. The macroscopic quantities (Temperature on figure 6 and Heat flux on figure 7) at the wall are very close.

Table 1: Characteristics of the simulation

gas	Argon
Prandtl number	$\frac{2}{3}$
molecular mass	$6.63\,10^{-26}kg$
Ma_∞	10.0
$Kn_\infty(Lref)$	0.05
ρ_∞	$5.636\,10^{-6}kg.m^{-3}$
T_∞	$198K$
Wall temperature	500 K
Boundary condition	purely diffusive

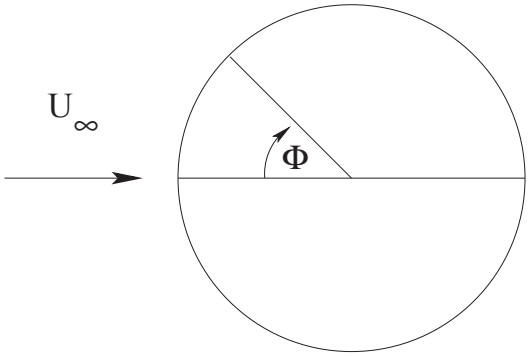

Figure 5: geometry of the simulation

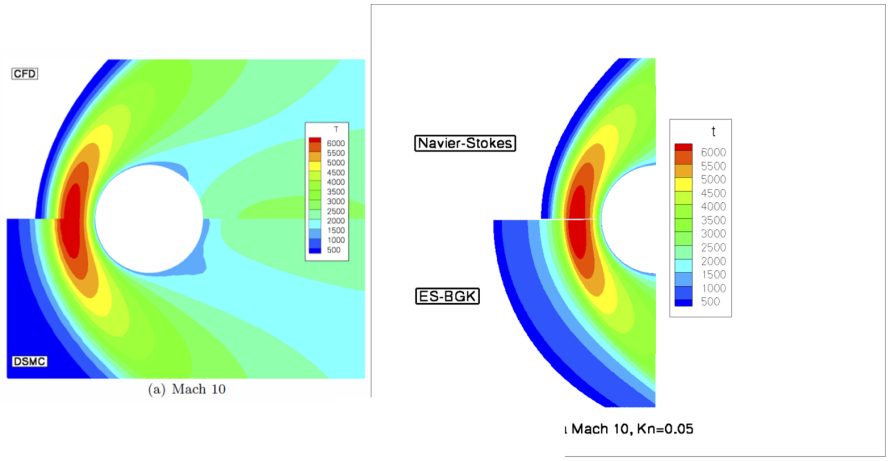

(a) Mach 10

Figure 6: Temperature fields with DSMC, BGK and two Navier-Stokes codes

DOI: 10.13009/EUCASS2017-601

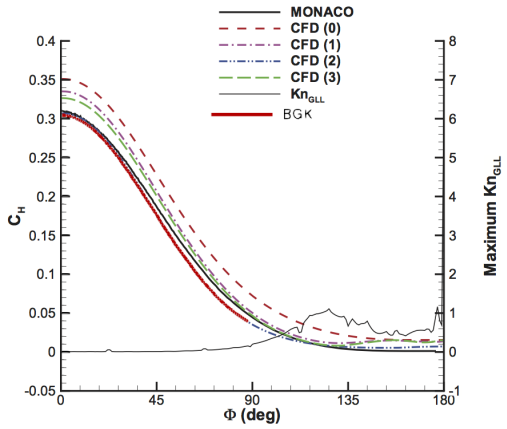

Figure 7: Heat flux with Monaco code, Navier-Stokes and our BGK code (red curve in solid line)

5. Comparison between Model and Measurement

5.1 Experimental data

The experiments were made at the MARHY facility (formerly named SR3) of the ICARE CNRS Laboratory at Orléans, France. MARHy is a Rarefied Hypersonic wind tunnel.[7] It is able to deliver a continuous Rarefied Flow with a large variety of experimental flow conditions: Mach numbers are contained between 0.6 and 21.1 and Reynolds numbers between 10^2 and 10^5 (with respect to a length of 10 cm). Since we had no previous experimental data, we decided to start with rather soft experimental conditions: the Mach number was equal to 4. Therefore, the flow is supersonic, but not hypersonic. The gas is air, and since it is not preheated, the temperature is about 70K in the flow. The pressure is low, in order to increase the mean free path of the molecules and the Knudsen number. The pressure condition that has been experimented in this study is P_∞=8Pa. The probe was a stainless steel sphere-cone, with a nose radius of 0.62mm and a length of 12.5mm. Knowing the pressure and temperature conditions, and the probe dimensions, one may calculate the Knudsen numbers. With the low pressure of 8Pa, Knudsen number has the value of Kn=8.5 10^{-4}. For objects of a metric size, this Knudsen number would be found at an altitude of approximately 80km. Even though we could be interested with more rarefied conditions, simulating higher altitudes, those experimental conditions are very interesting, since they are in the range where the comparison between the Navier-Stokes equations and the kinetic theory of gas is possible. The only measurements that were available during those first experiments are the pressure in the air flow. Pressure was measured with a Pitot tube, with the problems of measuring low pressure in a hypersonic flow.[1,14] So as to be able to measure the low pressures, the Pitot tube has a several millimeter diameter, and the rarefaction effects have to be taken into account. The effects are estimated prior to the experiment. Due to the supersonic air flow, a shock settles in front of the Pitot tube. Its effect also has to be taken into account while working on the measured pressure. Since the kinetic code computes the pressure within the gas flow, we chose to calculate a modified pressure, called P_P, so as to be able to directly compare the calculated and the measured pressures. This corrected pressure is calculated with the Rayleigh Pitot tube equation[1]

$$if Ma > 1 : P_p = P \times \frac{(\frac{\gamma+1}{2} Ma^2)^{\frac{\gamma}{\gamma-1}}}{(\frac{2\gamma}{\gamma+1} Ma^2 - \frac{\gamma-1}{\gamma+1})^{\frac{1}{\gamma-1}}} \tag{6}$$

With P being the local pressure in the gas flow, Ma the local Mach number (Ma>1) and et $\gamma = \frac{C_p}{C_v}$ for the concerned gas (in this experiment, gas is air then $\gamma = 1.4$).

5.2 Model parameters

The calculations were made with the ES-BGK kinetic code described in the first part of this paper. The model is 2D-axisymmetric, and this hypothesis has been confirmed by 3D pressure measurements in the flow. Mach number is set equal to 4, and the Knudsen number is calculated by the code, with use of the flow characteristics and the nose radius. The gas is polyatomic (air), and the chemistry is considered frozen. In these experimental conditions, the temperatures stay far below the dissociation temperature since they hardly reach 300K. As for the velocity is concerned, the infinite

DOI: 10.13009/EUCASS2017-601

velocity is 670m.s^{-1} and AMR velocity grid is described with 2148 points. The fluid domain is meshed with 200x60 meshes allocated within 4 blocks. The mesh has a better refinement close to the wall, and the characteristic size of the mesh is between 0.1μm and 11μm. In the flow far from the perturbations, the characteristic size of the mesh is close to 1cm.
With those parameters, the calculation last about 700s using 96 processors.

5.3 Kinetic code results

As was said earlier, the code to measurement comparisons will be made on the pressure measured by the Pitot tube, P_P. Those pressures are computed through the Rayleigh equation from the local pressures and Mach numbers. Figure 8 shows the computed Mach numbers in the air flow.

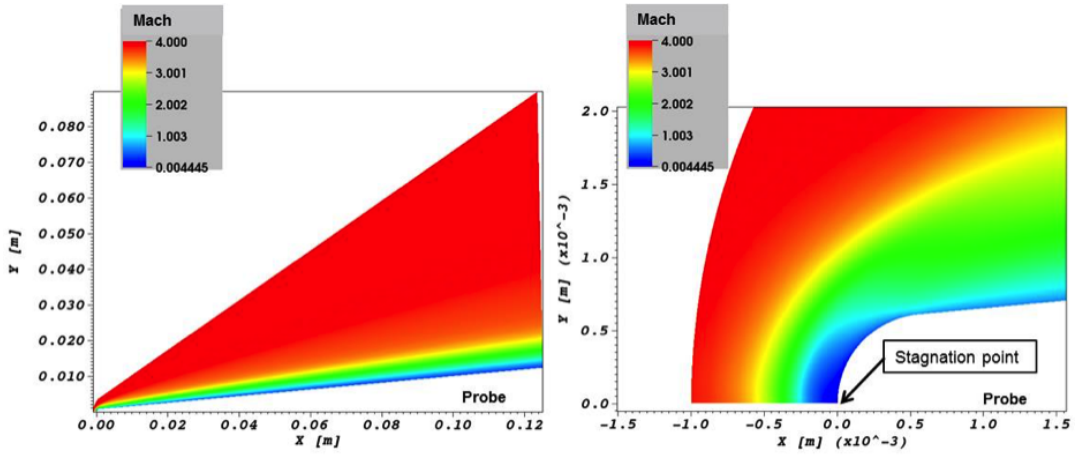

Figure 8: Computed (Kinetic code) Mach numbers with Ma_∞=4 and P_∞=7.9 Pa. Full mesh is shown on the left hand picture. Flow near the stagnation point is shown on the right hand picture

Figure 9 shows the computed pressures in the air flow.

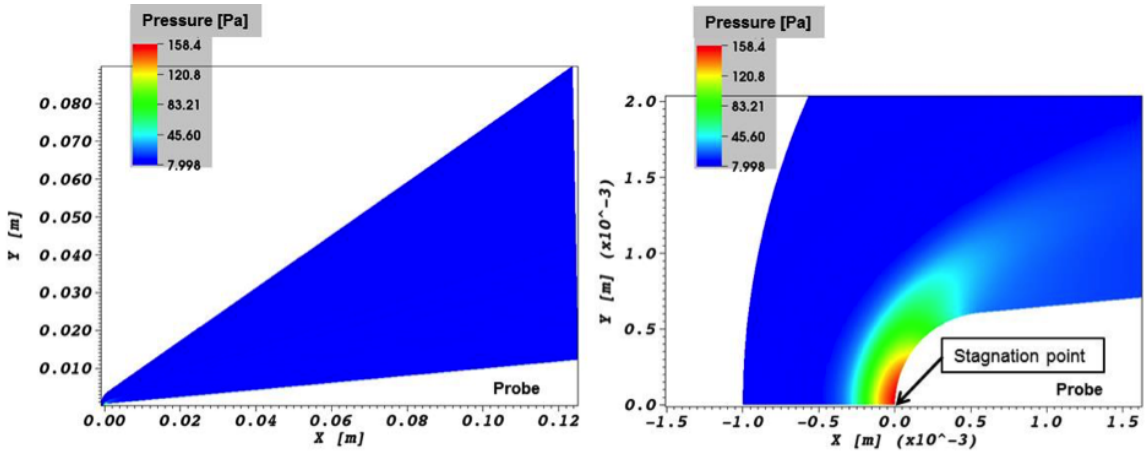

Figure 9: Computed (Kinetic code) pressure in the air flow with Ma_∞=4 and P_∞=7.9 Pa. Full mesh is shown on the left hand picture. Flow near the stagnation point is shown on the right hand picture

The shock is not quite visible, due to the rather low Mach number, and the rarefied regime. The highest pressure is computed at the stagnation point 158.4Pa when P_∞=8Pa.

5.4 Comparison computed and measured flow pressures

Those Mach and pressure fields can be used at each point of the mesh to compute the Pitot pressures, but we will compute and show the results only at the exact same locations where the measurement were made. Due to the rather

DOI: 10.13009/EUCASS2017-601

big size of the Pitot tube as compared to the size of the probe, it was not possible to measure the pressure close to the wall. Measurements were made all over a 2D-plane in the air flow, at several given abscissae x on Figure 8 or Figure 9 and with a 0.5mm step between two y-measurements. This yields to a big amount of data, and the comparisons shown in this study are for x=45mm and x=75mm only. Figure 10 shows the measured and computed Pitot pressures. The red line indicates the radius of the probe at the considered abscissa. The vertical blue line gives P_∞ for the Pitot Probe (Far from the shock wave, the real pressure is equal to $8Pa$ and the Mach number Ma to 4 so that the Pitot Pressure is equal to P_∞=168Pa).

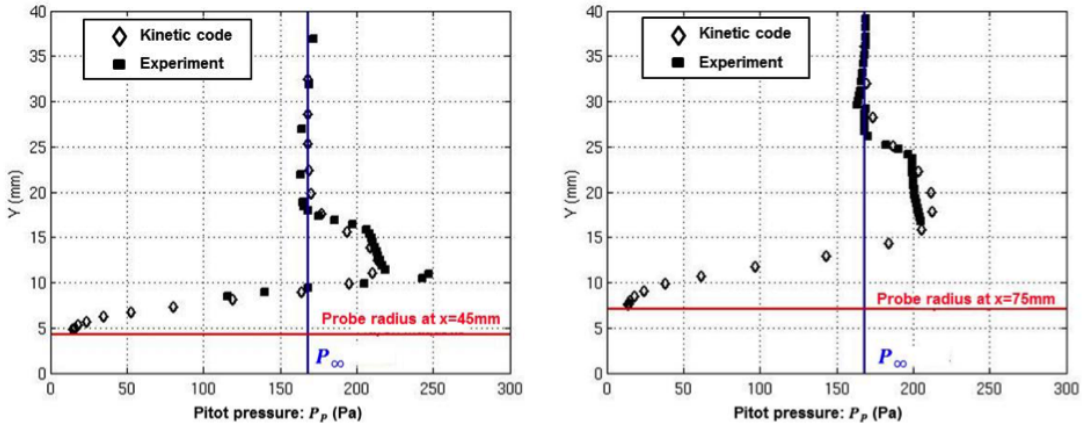

Figure 10: Computed (kinetic code) and measured Pitot pressures. x=45mm on the left hand side. x=75mm on the right hand side

The agreement between calculation and measurement is good, even if the large diameter of the Pitot tube does not allow one to do measurements closer to the wall. In fact, there are two experimental points at x=45mm and y=10mm that are quite different from the computed pressures. The difference may be due to interactions between the shock in front of the Pitot tube, and the boundary layer, which take place in the experiment, but are not taken into account in the model. Such interactions have to be further investigated.

5.5 Conclusion

One must keep in mind that this experiment was considered as the first step of a more complete study, with measurements at hypersonic velocities with high Mach numbers (Ma=20). The next probe should also be equipped with wall pressure measurement devices, and the awaited heat flux should make their measurement possible.

References

[1] J.D. Anderson. *Hypersonic and High Temperature Gas Dynamics*. McGraw-Hill series in aeronautical and aerospace engineering. American Institute of Aeronautics and Astronautics, 2000.

[2] P. Andries, P. Le Tallec, J.-P. Perlat, and B. Perthame. The gaussian-bgk model of boltzmann equation with small prandtl number. *European Journal of Mechanics - B/Fluids*, 19(6):813 – 830, 2000.

[3] K. Aoki, P. Degond, and L. Mieussens. Numerical simulations of rarefied gases in curved channels: thermal creep, circulating flow, and pumping effect. *Commun. Comput. Phys.*, 6:919–954, 2009.

[4] C. Baranger, J. Claudel, N. Hérouard, and L. Mieussens. Locally refined discrete velocity grids for deterministic rarefied flow simulations. *AIP Conference Proceedings*, 1501(1):389–396, 2012.

[5] C. Baranger, J. Claudel, N. Hérouard, and L. Mieussens. Locally refined discrete velocity grids for stationary rarefied flow simulations. *Journal of Computational Physics*, 257:572–593, 2014.

[6] G.A. Bird. *Molecular Gas Dynamics and the Direct Simulation of Gas Flows*. Oxford Science Publications, 1994.

DOI: 10.13009/EUCASS2017-601

[7] S. Coumar and V. Lago. Influence of mach number and static pressure on plasma flow control of supersonic and rarefied flows around a sharp flat plate. *Experiments in Fluids*, 58(6):74, 2017.

[8] L. Desvillettes and L. Mieussens. Etude de modélisation des écoulements raréfiés. *Internal publication*, 2014.

[9] B. Dubroca and L. Mieussens. A conservative and entropic discrete-velocity model for rarefied polyatomic gases. In *CEMRACS 1999 (Orsay)*, volume 10 of *ESAIM Proc.*, pages 127–139 (electronic). Soc. Math. Appl. Indust., Paris, 1999.

[10] L. H. Holway. Kinetic theory of shock structure using an ellipsoidal distribution function. In New York Academic Press, editor, *Rarefied Gas Dynamics, Vol. 1 (Proc. Fourth Internat. Sympos. Univ. Toronto, 1964)*, pages 193–215, 1966.

[11] A. J. Lofthouse, L. C. Scalabrin, and I. D. Boyd. Velocity slip and temperature jump in hypersonic aerothermodynamics. *Journal of thermophysics and heat transfer*, 22(1):38–49, 2008.

[12] L. Mieussens. Discrete Velocity Model and Implicit Scheme for the BGK Equation of Rarefied Gas Dynamics. *Math. Models and Meth. in Appl. Sci.*, 8(10):1121–1149, 2000.

[13] L. Mieussens. Discrete-velocity models and numerical schemes for the Boltzmann-BGK equation in plane and axisymmetric geometries. *J. Comput. Phys.*, 162:429–466, 2000.

[14] T. Ozawa, K. Fujita, and T. Suzuki. Development of an aerodynamic measurement system for hypersonic rarefied flows. *Review of Scientific Instruments*, 86(1):015105, 2015.

[15] V. A. Titarev. Efficient deterministic modelling of three-dimensional rarefied gas flows. *Communications in Computational Physics*, 12(1):162–192, 2012.

[16] H. C. Yee. *A Class of High-Resolution Explicit and Implicit Shock-Capturing Methods*. Von Karman Institute for Fluid Dynamics, Lectures Series, n^{o}4. Von Karman Institute for Fluid Dynamics, 1989.